Research in Astron. Astrophys. **2011** Vol. **11** No. **3**, 345–352
http://www.raa-journal.org *http://www.iop.org/journals/raa*

Research in Astronomy and Astrophysics

Potential generated by a massive inhomogeneous straight segment

Nour-Eddine Najid, El Haj Elourabi and Mohamed Zegoumou

Equipe Mécanique Statistique et Astronomie - Laboratoire de Physique Théorique et Appliquée
Université Hassan II Ain Chock- Faculté des Sciences Ain Chock BP 5366 Maârif Casablanca
Morocco; *ne.najid@gmail.com; elourabi2000@yahoo.fr; zagoumou1@hotmail.com*

Received 2009 December 25 ; accepted 2010 October 12

Abstract The discoveries of binary asteroids have opened an important new field of research concerning the calculation of potential generated by irregular bodies. Some of them have an elongated shape. A simple model to describe the motion of a test particle in that kind of potential requires consideration of a finite homogeneous straight segment. We construct this model by adding an inhomogeneous distribution of mass. To be consistent with the geometrical shape of the asteroid, we explore a parabolic profile of the density. We establish the closed analytical form of the potential generated by this inhomogeneous massive segment. The study of the dynamical behavior is fulfilled by the use of Lagrangian formulation, which allows us to calculate some two and three dimensional orbits.

Key words: asteroids — potential — inhomogeneous distribution

1 INTRODUCTION

The study of the potential generated by irregular bodies is an old problem. Space missions to minor bodies in the solar system and discoveries of binary asteroids have piqued new interest in this subject. Many attempts have been made to estimate the potential. Riaguas et al. (1999) proposed a homogeneous straight segment. Elipe & Lara (2003) described the motions around asteroid 433 Eros with the same homogeneous model. A harmonic polyhedron was used by Werner and Scheeres for asteroid 4769 Castalia in Werner & Scheeres (1997) and Werner (1994). Ellipsoids, material points and a segment of double material were used by Bartczak & Breiter (2003) and Bartczak et al. (2006), as the model of irregular elongated bodies. In our work, we propose a new method to model the potential generated by an elongated body. We consider a straight massive segment with variable density. To be consistent with the geometrical aspect of the asteroid, we use a parabolic profile. Our work generalizes that of Riaguas et al. (1999). In Section 2, we establish a closed form of the potential generated by an inhomogeneous massive segment. In Section 3, we study the dynamical behavior of a test particle in the field of the straight segment. We continue in Section 4 by numerically solving the differential equations of motion. In this section we also plot some orbits in two and three dimensions. In Section 5 we draw conclusions of our study.

2 POTENTIAL CALCULATION

We consider a straight segment of length $2l$ and total mass M, centered at O, the origin of the Ox axis . The density of this segment is given by

$$\lambda(x) = -ax^2 + b, \tag{1}$$

in which a and b are positive constants related by $a < \frac{b}{l^2}$ and $M = -\frac{2}{3}al^3 + 2bl$. At the point P, the gravitational potential generated by the segment is:

$$U(P) = -G \int \frac{dm}{r}, \tag{2}$$

where G is the gravitational constant and r is the distance between P and the infinitesimal mass dm located at H with abscissa x_H in the segment as shown in Figure 1. We define $\nu = \frac{1}{2}(1 + \frac{x_H}{l})$ as a new variable of integration, where $0 \leq \nu \leq 1$. Here r is given as in Riaguas et al. (1999) by

$$r^2 = r_1^2 + 4l^2\nu^2 + \nu\left(r_2^2 - r_1^2 - 4l^2\right), \tag{3}$$

where r_1 and r_2 are the distances from P to the end points of the segment, and

$$dm = \lambda(x_H)dx_H,$$

$$dm = 2l(-4al^2\nu^2 + 4al^2\nu + b - al^2)d\nu. \tag{4}$$

Equation (2) yields

$$U(r_1, r_2) = 4al^2G \int_0^1 \frac{\nu^2 - \nu - \frac{b-al^2}{4al^2}}{\sqrt{\nu^2 + \nu\left(\frac{r_2^2-r_1^2-4l^2}{4l^2}\right) + \frac{r_1^2}{4l^2}}} d\nu. \tag{5}$$

After some laborious calculation and simplification, we obtain the closed expression of the potential generated at P

$$U(r_1, r_2) = \frac{G}{32l^2}\left\{\begin{array}{l} 16al^3\left(r_2 + r_1\right) + 12al\left(r_2 - r_1\right)\left(r_1^2 - r_2^2\right) + \\ \left[\begin{array}{l} 8al^2\left(r_2 + r_1\right)^2 - 16al^2 r_1 r_2 \\ -3a\left(r_1 - r_2\right)^2\left(r_2 + r_1\right)^2 - 16al^4 + 32bl^2 \end{array}\right] \ln\left(\dfrac{r_2 + r_1 - 2l}{r_2 + r_1 + 2l}\right) \end{array}\right\}$$

by denoting

$$\begin{cases} s = r_2 + r_1, \\ d = r_1 - r_2, \\ p = r_2 r_1. \end{cases}$$

The last expression reduces to

$$U(P) = -\frac{G}{32l^2}\left\{12alsd^2 - 16al^3s + \left[8l^2a\left(s^2 - 2p\right) - 3as^2d^2 - 16l^4a + 32bl^2\right]\ln\left(\frac{s + 2l}{s - 2l}\right)\right\}. \tag{6}$$

Equation (6) represents the gravitational potential generated by an inhomogeneous straight segment with a quadratic density profile. The case of constant density (Riaguas et al. 1999) is a particular case of Equation (6), if we put $a = 0$ and $b = \frac{M}{2l} = \lambda$. We obtain expression (1) in Riaguas et al. (1999).

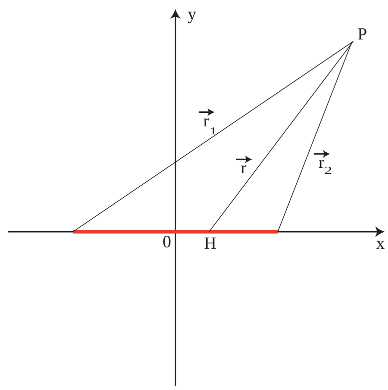

Fig. 1 Straight segment.

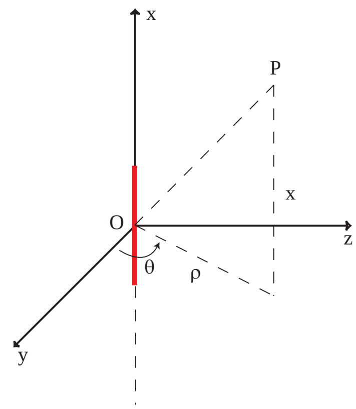

Fig. 2 Sidereal reference and the cylindrical coordinates.

3 DYNAMICAL STUDY

We plan to study the dynamical behavior of a test particle, with unit mass, located at P in the field of the inhomogeneous straight segment. $R(O, x, y, z)$ is the sidereal reference frame, with the cylindrical coordinates $(\rho,\ \theta,\ x)$ as shown in Figure 2.

The Lagrangian of the test particle is given by

$$L = \frac{1}{2}\left(\dot{\rho}^2 + \rho^2\dot{\theta}^2 + \dot{x}^2\right) - U(r_1, r_2), \tag{7}$$

where

$$\begin{cases} r_1 = \sqrt{\rho^2 + (x+l)^2}, \\ r_2 = \sqrt{\rho^2 + (x-l)^2}. \end{cases}$$

The differential equations of motion are then

$$\ddot{\rho} = \rho\dot{\theta}^2 + \frac{G}{32l^2p}\left\{\begin{array}{l} 32al^2p\rho\ln\left(\dfrac{s+2l}{s-2l}\right) - 4al\rho s\left(3d^2+4l^2\right) \\ -\dfrac{4l\rho s}{s^2-4l^2}\left[8l^2a\left(s^2-2p\right) - 3as^2d^2 - 16l^4a + 32bl^2\right] \end{array}\right\}. \tag{8}$$

$$\ddot{x} = \frac{Ga}{16l^2p}\left\{\begin{array}{l} 2l\left(xs-ld\right)\left(3d^2-4l^2\right) + 12lsd\left(ls-xd\right) \\ +\left[s\left(xs-ld\right)\left(8l^2-3d^2\right) - 8l^2x\left(s^2-2p\right) + 8l^3sd - 3s^2d\left(ls-xd\right)\right]\ln\left(\dfrac{s+2l}{s-2l}\right) \\ -\dfrac{2l\left(xs-ld\right)}{s^2-4l^2}\left[8l^2\left(s^2-2p\right) - 3s^2d^2 - 16l^4 + \dfrac{32bl^2}{a}\right] \end{array}\right\}, \tag{9}$$

$$\rho^2\dot{\theta} = \Lambda = \text{const.} \tag{10}$$

Again we can check the case of constant density, and we obtain equation (3) as in Riaguas et al. (1999).

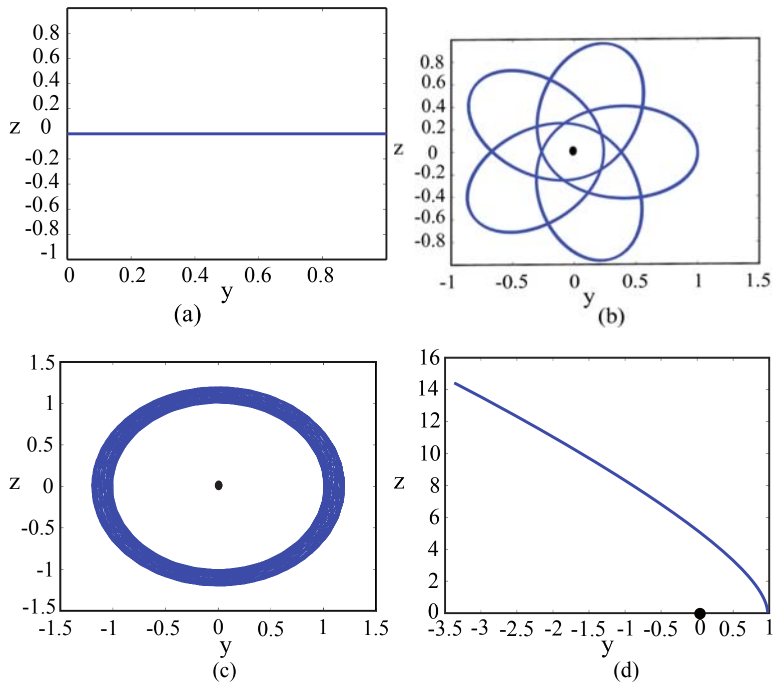

Fig. 3 Trajectories in the equatorial plane yz.

4 NUMERICAL INTEGRATION

To gain deep insight about the dynamical behavior of the test particle in the field of the inhomogeneous straight segment, we have to solve Equations (8), (9) and (10). In this system of differential equations, the unknown variables are ρ, θ and x. We derive some curves, both in the plane and in the three dimensional space. To aid in a more accurate interpretation of these results, we can study the behavior of the Poincaré surface of the section.

4.1 Study of the Resulting Trajectories

A- Equatorial plane

In the plane (yOz), only ρ and θ are variables while x is kept constant at zero.

- Figure 3(a) corresponds to free fall with $\rho_0 = 1, \theta_0 = 0, \dot{\rho}_0 = 0$ and $\dot{\theta}_0 = 0$.
- Figure 3(b) $\rho_0 = 1, \theta_0 = 0, \dot{\rho}_0 = 0$ and $\dot{\theta}_0 \neq 0$.
- Figure 3(c) $\rho_0 = 1, \theta_0 = 0, \dot{\rho}_0 = 0$ and $\dot{\theta}_0 \neq 0$, the same as in Figure 3(b) with increased time of integration. We notice that the test particle evolves along an orbit confined between two trajectories limited by the minimum and maximum values of ρ.

  We conclude that the segment behaves as if the whole mass is located at its center. We have a central field and the motion is in the plane. If we continue to increase $\dot{\theta}_0$, the permitted zone of the orbit of the test particle shrinks. Beyond a critical value $\dot{\theta}_{0c}$, the test particle escapes (Fig. 3(d)).

  By plotting different orbits of the test particle, we show that $\dot{\theta}_{0c}$ depends on $\dot{\rho}_0$.

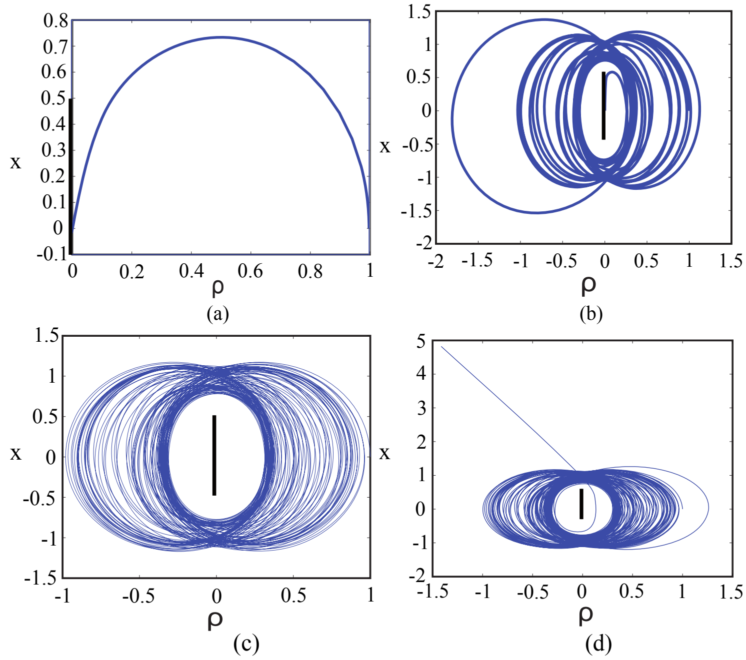

Fig. 4 Trajectories in the meridian plane ρx.

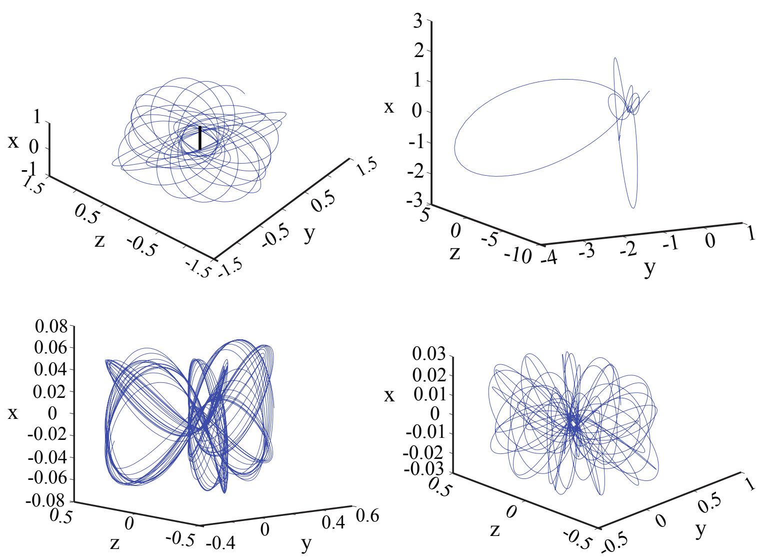

Fig. 5 Trajectories in the space xyz.

B- Meridian plane

In Figure 4(a)–(d), we have $\rho_0 = 1$, $\dot{\rho}_0 = 0$ and $\dot{x}_0 \neq 0$. For a small value of $\dot{x}_0$, we obtain a collision as shown in Figure 4(a) and (b). By increasing the value of $\dot{x}_0$, the test particle spends more time around the segment without any collision (Fig. 4(c)). At the end, $\dot{x}_{0c}$ gives an escape (Fig. 4(d)).

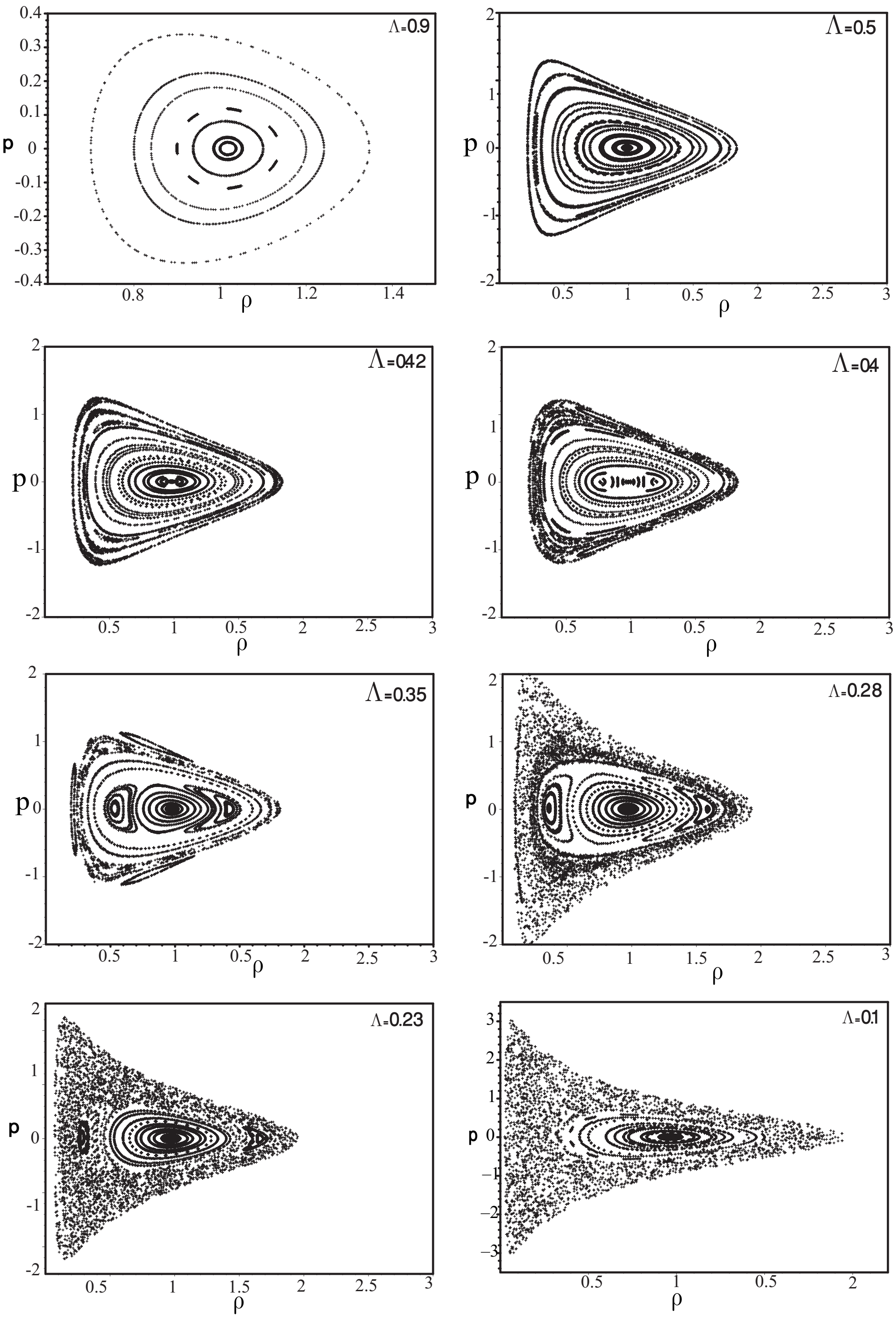

Fig. 6 Poincaré sections for different values of Λ.

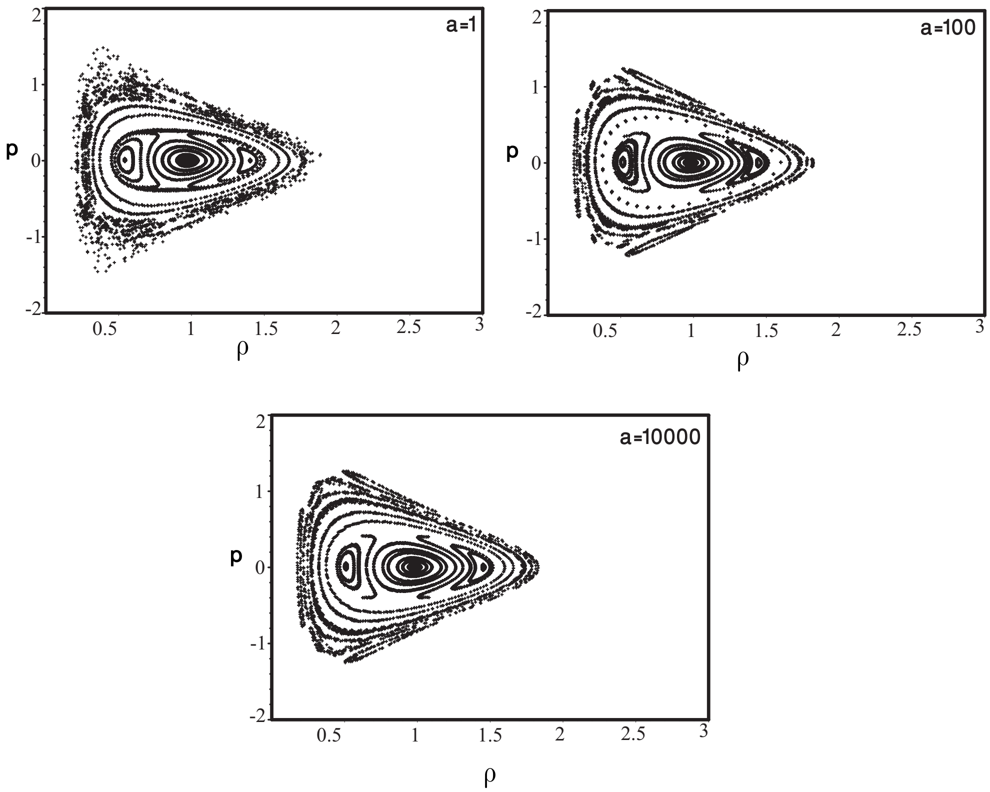

Fig. 7 Poincaré sections for different values of a and b.

C-In the space

Figure 5 gives some orbits in the space corresponding to different initial conditions. We notice, from a qualitative point of view, many types of behaviors, especially the cases where the test particle is either confined or unconfined.

4.2 Poincaré Surface of Section

To study the dynamical behavior of the system, we plot the Poincaré surface of this section. Equation (10) shows that Λ is an integral, which leads us to restrict the study of the motion to the plane $(Ox\rho)$. Equation (7) shows that the system is autonomous, hence the energy h is

$$h = \frac{1}{2}\left(\dot{\rho}^2 + \dot{x}^2 + \frac{\Lambda^2}{\rho^2}\right) + U(P),$$

which is an integral.

We define the surface of the section as $h = \mathrm{const.}$, $x = 0$, and $\dot{x} > 0$. We then plot the points $(\rho, \dot{\rho})$ in this plane. Figure 6 shows the Poincaré surfaces of the section for an elongated inhomogeneous straight segment in which $a = 10$ and $b = 3.50$ with $h = -0.5$ and decreasing values of Λ.

From $\Lambda = 0.44$ to 0.9, the section shows the same behavior as a homogeneous straight segment (Riaguas et al. 1999). By decreasing the value of Λ, the topology of the surface is subjected to an important change.

For the value $\Lambda = 0.44$, the limit cycles disappear and bifurcate. In between two elliptic points, there is a hyperbolic point. The bifurcation continues to evolve until Λ reaches 0.35 where the hyperbolic point is transformed to an elliptic one and the elliptic points to two hyperbolic points.

In the last transformation, we notice a great difference between the homogeneous and nonhomogeneous bodies. Indeed, in our model, we establish the existence of two symmetric islands about the $\rho - axis$ and a central island. Below $\Lambda = 0.30$, the three islands disappear and the region of chaotic behavior is wider. Finally for $\Lambda = 0.1$, the structure returns to the homogeneous straight segment (Riaguas et al. 1999).

The Poincaré surface of the section in Figure 6 gives an overview of the structure of the dynamical behavior of the test particle. Among the various results, we find those corresponding to the numerical integrations shown in Figures 3, 4 and 5.

To show the effect of inhomogeneity in the body, we plot the surface of the section with $\Lambda = 0.35$ and $h = -0.5$ (Fig. 7). For weak values of a, the Poincaré surface of the section shows the same dynamical behavior. When we increase the values of a, we notice that the chaotic zones shrink and some islands appear. From $a = 100$, the limit cycles are transformed to resonant orbits, but subsequently return to limit cycles for high values of a.

5 CONCLUSIONS

In this work, we established a new analytical expression for the potential generated by a straight segment with a quadratic profile of its density. For this expression of the potential, we found periodic orbits, and their associated stability or bifurcation. After finding these results of the dynamical behavior of a test particle in the field of that segment, which is fixed in space, in the future, we plan to study the case where the segment is rotating. In this case, the effect of rotation and gravitation gives rise to relative equilibrium positions for the test particle in the homogeneous case as in Elipe et al. (1999). In our model of the nonhomogeneous straight segment, we have developed a new analytical way to calculate the result. In this situation, we derived the equations of motion governing the dynamical behavior of the system, and studied the effect of inhomogeneity under the new conditions of equilibrium points.

Acknowledgements N-E Najid thanks A. Riaguas for sending the original article (Riaguas et al., 1999).

References

Bartczak, P., & Breiter, S. 2003, Celestial Mechanics and Dynamical Astronomy, 86, 131
Bartczak, P., Breiter, S., & Jusiel, P. 2006, Celestial Mechanics and Dynamical Astronomy, 96, 31
Elipe, A., & Lara, M. 2003, The journal of Astronotical Sciences, 51, 391
Elipe, A., Lara, M., & Riaguas, A. 1999, RBCM-J. of the Braz. Soc. Mechanical Sciences, XXI, 198
Riaguas, A., Elipe, A., & Lara, M. 1999, Celestial Mechanics and Dynamical Astronomy, 73, 169
Werner, R. A. 1994, Celestial Mechanics and Dynamical Astronomy, 59, 253
Werner, R. A., & Scheeres, D. J. 1997, Celestial Mechanics and Dynamical Astronomy, 65, 313